J Therm Anal Calorim (2009) 98:533–537
DOI 10.1007/s10973-009-0298-7

Thermal stability, decomposition and glass transition behavior of PANI/NiO composites

Yanni Qi · Jian Zhang · Shujun Qiu · Lixian Sun · Fen Xu · Min Zhu · Liuzhang Ouyang · Dalin Sun

Received: 21 August 2008 / Accepted: 30 January 2009 / Published online: 25 July 2009

Abstract Polyaniline/NiO (PANI/NiO) composites were synthesized by in situ polymerization at the presence of HCl (as dopant). FTIR, TEM and XRD were used to characterize the composites. Thermogravimetry (TG)–mass spectrometer (MS) and temperature modulated differential scanning calorimetry (TMDSC) were used to study the thermal stability, decomposition and glass transition temperature (T_g) of the composites, respectively. FTIR and XRD results showed that NiO nanoparticles connected with PANI chains in the PANI/NiO composites. TEM results exhibited that the morphologies of PANI/NiO composites were mostly spherical, which were different from the wirelike PANI. TG–MS curves indicated that the products for oxidative degradation of both PANI and PANI/NiO composite were H_2O, CO_2, NO and NO_2. TG curves showed that with NiO contents increased in PANI/NiO composites, thermal stability of PANI/NiO composites increased firstly and then decreased when the NiO content was higher than 66.2 wt%. T_g of PANI/NiO composites also increased from 163.19 to 252.36 °C with NiO content increasing from 0 to 50 wt%, and then decreased with NiO content increasing continuously.

Keywords PANI/NiO composite · Thermal stability · TG–MS analysis · T_g

Y. Qi · J. Zhang · S. Qiu · L. Sun (✉)
Materials and Thermochemistry Laboratory, Dalian Institute of Chemical Physics, Chinese Academy of Sciences, 457 Zhongshan Road, Dalian 116023, People's Republic of China
e-mail: lxsun@dicp.ac.cn

F. Xu (✉)
Faculty of Chemistry and Chemical Engineering, Liaoning Normal University, Dalian 116023, People's Republic of China
e-mail: xufen@lnnu.edu.cn

M. Zhu · L. Ouyang
School of Material Science and Engineering, South China University of Technology, Guangzhou 510640, People's Republic of China

D. Sun
Department of Material Science, Fudan University, Shanghai 200433, People's Republic of China

Introduction

Conducting polymer was not of major interest until about 1977, when conductivity of polyethyne was discovered [1]. Compared with other conductive polymer, polyaniline (PANI) attracted much attention for its easy preparation, environmental stability, special doping mechanism and its potential applications in electronic devices, batteries, biosensors. etc. [2–4]. However, lower conductivity (as metal as concerned), poorly thermal stability and infusibility of PANI limited its application field. To resolve some of these problems, composites composed of PANI and inorganic nanoparticles were prepared to obtain special characteristics from nanoparticles [5–7]. Among multitudinous types of inorganic nanoparticles, metal oxides are mostly thermally stable, which would improve thermal stability of PANI; furthermore, widen the application field of it.

In [8–11], composites composed of PANI and metal oxide nanoparticles (like Co_3O_4, montmorillonite, γ-Al_2O_3 and α-Al_2O_3) were prepared and the thermal properties of the composites were studied. The results indicated that more thermally stable nanoparticles improved the thermal properties of PANI by the interaction between them. NiO nanoparticles, which also have excellent thermal stability, were capable of improving the thermal stability of PANI [12]. While, if the content of impurity in NiO nanoparticles was

high enough to make its thermal stability lower than PANI. Whether the thermally stable behavior of PANI/NiO composite would exist or the thermal stability would lower than PANI. In this article, we chose above type of NiO nanoparticles and synthesized PANI/NiO composites by in situ polymerization. XRD, FTIR and TEM were used to characterize PANI/NiO composites. The thermal properties including thermal stability and thermal decomposition of PANI/NiO composites were studied by TG–MS analysis. And T_g of the composites were measured by TMDSC technique.

Experimental

Materials

Aniline obtained from Shenyang Federation Reagent Factory was purified twice by vacuum distillation and was stored in refrigerator before use. Ammonium persulfate ($(NH_4)_2S_2O_8$, APS) used as an oxidant was purchased from Tianjin Jizhun Chemical reagent Co. Ltd, hydrochloric acid (HCl) was provided by Harbin Chemical Reagent Co. and NiO nanoparticles with particle size smaller than 100 nm was obtained from Nanjing Haitai Technology Nano-Co. Ltd. All chemical reagents were of analytical grade.

Preparation of PANI/NiO composites

PANI/NiO composite was synthesized by in situ polymerization, which was similar to [10]. Firstly, a known volume of aniline was injected into 10 mL of 2 M HCl aqueous solution, stirred for 0.5 h. Then NiO nanoparticles were added into the above solution with stirring and ultrasonic action to reduce the aggregation of NiO nanoparticles. After 5 h, a known amount of APS (dissolved in 10 mL deionized water) was dropped into the above solution with stirring. The reaction mixture was continuously stirred at room temperature for 12 h. The production was then washed thoroughly with methanol and deionized water repeatedly till the filtrate was colorless. Finally, the product was dried in vacuum at 80 °C for 24 h. For each experiment, the molar ratios of aniline to HCl and to APS were retained at 1:0.5 and 1:1, respectively.

Instrumental methods

XRD patterns of NiO, pure PANI and PANI/NiO composites were recorded on a PANalytical X′Pert PRO diffractometer fitted with Cu K_α radiation ($\lambda = 1.5404$ nm) at 40 kV and 40 mA, with a scanning speed of 10° min^{-1}. FTIR absorption spectra of pure PANI and PANI/NiO composites were performed on a Bruck Equinox 55 spectrophotometer in the wavelength range of 4000–400 cm^{-1}. The specimen substrate was a KBr disc. The morphologies of PANI/NiO composites were measured on TEM instrument of JEM-2000EX.

Thermal properties

The thermal stability decomposition of pure PANI, NiO nanoparticles and PANI/NiO composites were performed on a thermogravimetric analyzer DT-20B instrument coupled with an IPI (In process instruments) GAM 200 mass spectrometer. TG curves were obtained under air atmosphere at a heating rate of 10 °C min^{-1} from room temperature to 800 °C with flow rate of 30 mL min^{-1}. The mass to charge ratios selected for analysis were 18, 28, 30, 44 and 46 amu, which indicated the mass fragments of H_2O, N_2, NO, CO_2 and NO_2, respectively. A 0.2-s acquisition time for each mass unit was set. T_g of pure PANI and PANI/NiO composites were measured by temperature modulated differential scanning calorimetry (TMDSC) on a Q1000 from TA Instruments in a temperature range from 50 to 250 °C, at a heating rate of 3 °C min^{-1}. Nitrogen was used to be the protective gas. The temperature scale of the instrument was calibrated at a heating rate of 20 °C min^{-1} with the melting points of indium. The energy scales were calibrated with the heat of fusion of indium. Crimp aluminum alloy pans were used under dry nitrogen flow (50 mL min^{-1}). Standard modulation conditions were amplitude A_T of 0.5 °C and a period of 40 s.

Results and discussion

Structure of PANI/NiO composites

Figure 1 shows the XRD patterns of PANI, NiO nanoparticles and PANI/NiO composite [20.1/79.9 (mass/mass)]. It can be seen that in the range of 2θ from 5 to 75°, the PANI exhibited two characteristic peaks at about 20 and 26°, which indicated that pure PANI had crystallinity to a certain extent. NiO nanoparticles with hexagonal structure showed four broad peaks at about 16, 35, 60 and 71° for its nano-structure. The PANI/NiO composite [20.1/79.9 (mass/mass)] integrated peaks of PANI and NiO nanoparticles. While, the characteristic peaks of PANI shifted to higher angles in the XRD pattern of PANI/NiO composite [20.1/79.9 (mass/mass)] for the interaction of PANI chains and NiO nanoparticles.

FTIR spectra of (a) PANI, (b) NiO nanoparticles and (c) PANI/NiO composite [20.1/79.9 (mass/mass)] are shown in Fig. 2. From FTIR spectrum of NiO nanoparticles, it can be seen that the characteristic peak at about wave number 717 cm^{-1} was ascribed to the vibration of NiO crystal lattice. And the peaks at about 836, 1409 and 1436 cm^{-1}

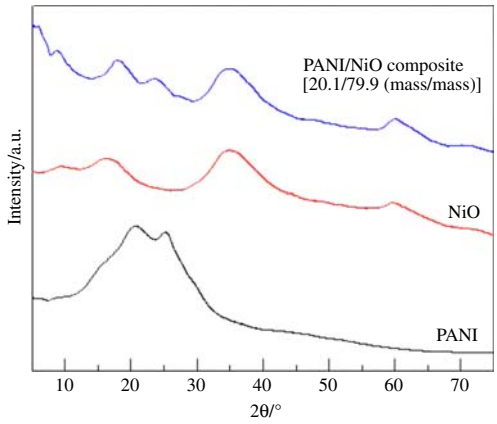

Fig. 1 XRD patterns of PANI, NiO nanoparticles and PANI/NiO composite [20.1/79.9 (mass/mass)]

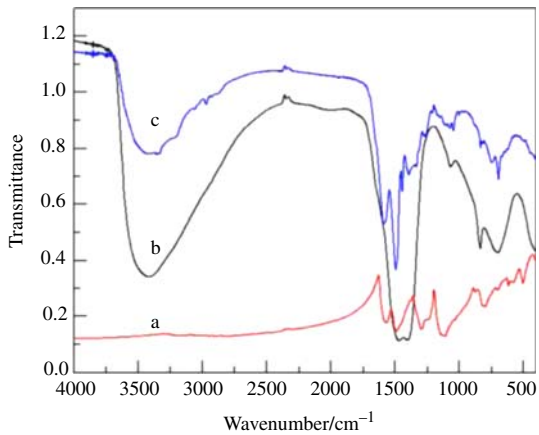

Fig. 2 FTIR spectra of (*a*) PANI, (*b*) NiO nanoparticles and (*c*) PANI/NiO composite [20.1/79.9 (mass/mass)]

were attributed to the impurity in NiO nanoparticles. Absorption bands at 1130, 1295, 1492 and 1572 cm^{-1} of PANI were in well accord with [13]. In FTIR spectrum of PANI/NiO composite [20.1/79.9 (mass/mass)], characteristic peaks represented PANI at 1068, 1271, 1490 and 1597 cm^{-1} were similar with those of pure PANI. While, the peaks position shifted a little for the interaction between PANI chains and NiO nanoparticles. The peak of NiO was also existed in PANI/NiO composite [20.1/79.9 (mass/mass)] spectrum.

Figure 3 shows the TEM images of (a) PANI, (b) NiO nanoparticles and (c) PANI/NiO composite [20.1/79.9 (mass/mass)]. Morphology of pure PANI was wirelike or tubular. And the diameter and length were about 100 and 500 nm, respectively. NiO nanoparticles were mostly spherical with diameter about 50 nm. PANI/NiO composite [20.1/79.9 (mass/mass)] exhibited similar shape with that of NiO nanoparticles except part aggregation. The diameter was about 100 nm. It might be a result of aniline polymerization and growth encircled the NiO nanoparticles.

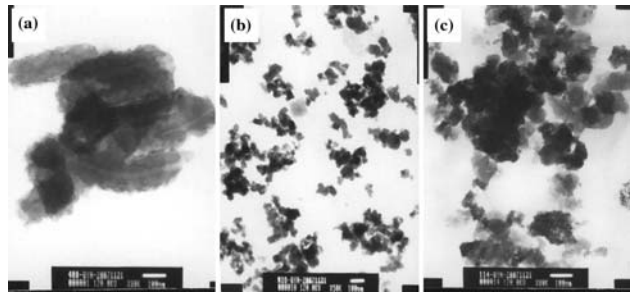

Fig. 3 TEM images of (**a**) PANI, (**b**) NiO nanoparticles and (**c**) PANI/NiO composite [20.1/79.9 (mass/mass)]

NiO content in PANI/NiO composites

NiO content in PANI/NiO composites can be calculated from TG curves of PANI/NiO composites. Figure 4 shows TG curves of PANI, NiO nanoparticles and PANI/NiO composites. It can be seen that PANI showed total mass loss of ca. 97.7% from room temperature to 700 °C. In the same temperature, the total mass loss of NiO nanoparticles was ca. 35.9%. And TG curve of PANI/NiO composite [50/50 (mass/mass)] gave a mass loss of 85.9%. So, the content of PANI in this composite was (85.9 − 35.9) = 50%. The content of NiO in the composite was (100 − 50) =50%.

Thermal stabilities and decomposition of PANI/NiO composites

Figure 5 shows TG–MS diagrams of PANI, NiO nanoparticles and PANI/NiO composite [20.1/79.9 (mass/mass)]. In Figs. 4 and 5, the TG curve of PANI showed two steps of mass loss. The first one was from ca. 50 to ca. 152 °C. In MS curves of Fig. 5, the peak at ca. 110 °C in the 18 amu curve can be seen, which indicated that this step of mass loss was due to the elimination of H_2O [13, 14].

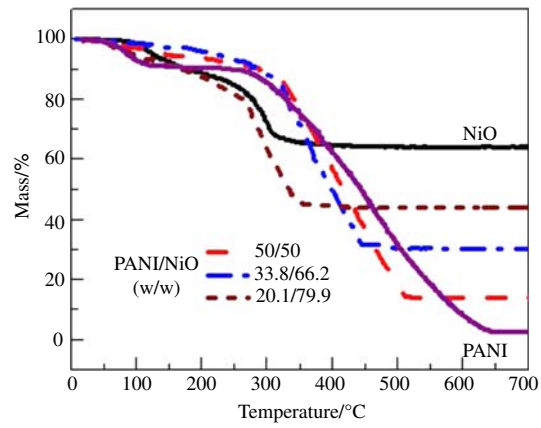

Fig. 4 TG curves of PANI, NiO nanoparticles and PANI/NiO composites

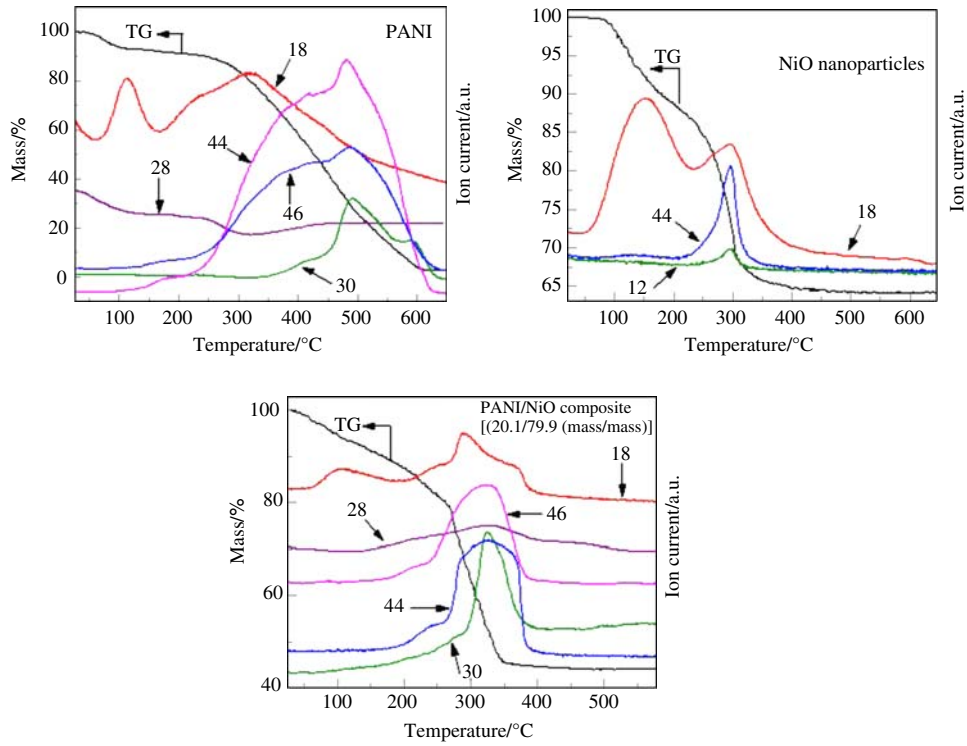

Fig. 5 TG–MS diagrams of PANI, NiO nanoparticles and PANI/NiO composite [20.1/79.9 (mass/mass)]

The second step of mass loss was from ca. 240 to ca. 620 °C. In this temperature range, the peaks of MS curves for 18, 30, 44 and 46 amu mass fragments can be observed, which indicated that the products of this step including H_2O, NO, CO_2 and NO_2, respectively [15, 16]. It was due to the oxidative degradation of PANI chains [17, 18]. In the MS diagram of PANI, the decrease in 28 amu mass fragment curve meant that N_2 likewise participated in the reaction of PANI degradation. NiO nanoparticles also had two steps of mass loss. The first one was from ca. 78 to ca. 187 °C for the H_2O evaporation (the peak in 18 amu curve can be seen in Fig. 5). The second step of mass loss was ascribed to the oxidation of impurity in NiO nanoparticles, which was from 187 to 340 °C, mostly for the oxidation of hydrocarbon because of the changes on the 18 and 44 amu curves. PANI/NiO composite [20.1/79.9 (mass/mass)] showed two steps mass loss like pure PANI and NiO nanoparticles. From the MS curves of Fig. 5, it can be seen that the curves of 18, 30, 44 and 46 amu mass fragments were similar with that of pure PANI. Therefore, the first step of mass loss to ca. 275 °C was caused by both of H_2O elimination and impurity oxidation in NiO nanoparticles. And the second step of mass loss was mostly ascribed to the degradation of PANI chains. In the MS diagram, the peak in 28 amu curve indicated that the content of CO_2 produced by PANI degradation was higher than the content decrease in N_2.

Temperatures corresponding to the mass loss of both 10% (T_{10}) and 20% (T_{20}) in TG curves represent the thermal stability of PANI, NiO nanoparticles and PANI/NiO composites. Table 1 lists T_{10} and T_{20} obtained from Fig. 4. With augment of NiO content, T_{10} and T_{20} increased firstly and then decreased. When NiO content was lower than 66.2%, T_{10} and T_{20} of PANI/NiO composite was higher than that of pure PANI (249.1 and 328.7, respectively). While, when the content of NiO was higher than 79.9%, T_{10} and T_{20} of PANI/NiO composite was lower than that of NiO itself (178.2 and 276.1 °C, respectively). It indicated that suitable amount of impure NiO nanoparticles improved the thermal stability of PANI.

T_g of PANI/NiO composites

TMDSC curves of PANI and PANI/NiO composites are shown in Fig. 6. T_g of PANI and PANI/NiO composites were evaluated from Fig. 6 and the data were listed in Table 1. From Table 1 and Fig. 6, it can be seen that with NiO content increasing from 0 to 50%, T_g of PANI/NiO

Table 1 T_{10}, T_{20} in TG and T_g in TMDSC

Sample	NiO content (%)	T_{10} (°C)	T_{20} (°C)	T_g (°C)
1	0	249.1	328.7	163.19
2	50	288.6	341.4	252.36
3	66.2	282.0	331.3	172.66
4	79.9	166.8	261.7	138.76
5	100	178.2	276.1	–

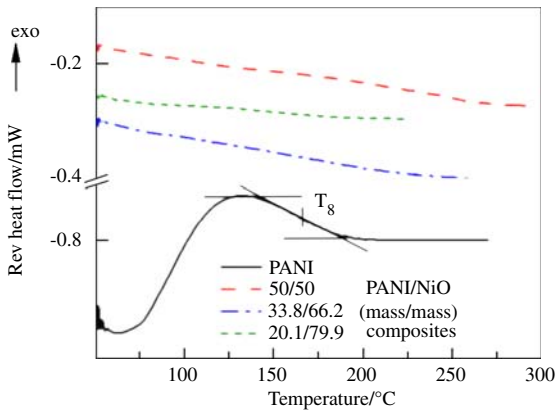

Fig. 6 TMDSC curves of PANI and PANI/NiO composites

composites increased from 163.19 to 252.36 °C. Whereas, with NiO content increasing continuously to 79.9%, T_g of PANI/NiO composites decreased. It may be because that when NiO content was lower than 50%, the nanoparticles could interact with PANI chains, which restricted the thermal motion of PANI and the T_g of PANI/NiO composites increased. While, when NiO content was higher than 50% in the composite, the aggregation of NiO nanoparticles occurred, the interaction between PANI and NiO weakened. So the free PANI chains increased and the T_g decreased.

Conclusions

PANI/NiO composites were prepared by in situ polymerization. XRD and FTIR results indicated that NiO nanoparticles influenced the structure of PANI through the interaction between PANI chains and NiO nanoparticles. Morphology of PANI/NiO composite was similar with that of NiO nanoparticles. TG–MS analysis showed that the products for oxidative degradation of both PANI and PANI/NiO composite were H_2O, CO_2, NO and NO_2. TG and TMDSC curves indicated that with NiO content increasing from 0 to 50%, thermal stability and T_g of PANI/NiO composites increased. While, the continuing increase (from 50 to 79.9%) in NiO content decreased the thermal stability and T_g of PANI/NiO composites for the aggregation of NiO nanoparticles.

Acknowledgements The authors gratefully acknowledge the financial support for this work from the National Natural Science Foundation of China (No. 2083309, 20873148, 50671098 and U0734005) and the National High Technology Research and Development Program (863 Program) of China (No. 2007AA05Z115 and 2007AA05Z102).

References

1. Shirakawa H, Louis EJ, Macdiarmid AG, Chiangand CK, Heeger AF. Synthesis of electrically conducting organic polymers: halogen derivatives of polyacetylene, $(CH)_x$. J Chem Soc Chem Commun. 1977;16:578–580.
2. Heeger AJ. Semiconducting and metallic polymers: the fourth generation of polymeric materials (Nobel Lecture). Angew Chem Int Ed. 2001;40:2591–611.
3. Li WG, Jia QX, Wang HL. Synthesis and characterisation of electroactive polyamide with amine-capped aniline. Polymer. 2006;47:23–6.
4. Xian YZ, Hu Y, Liu F, Xian Y, Wang HT, Jin LT. Glucose biosensor based on Au nanoparticles–conductive polyaniline nanocomposite. Biosens Bioelectron. 2006;21:1996–2000.
5. Schnitzler DC, Meruvia MS, Hummelgen IA, Zarbin AJG. Preparation and characterization of novel hybrid materials formed from $(Ti,Sn)O_2$ nanoparticles and polyaniline. Chem Mater. 2003;15:4658–65.
6. Houdayer A, Schneider R, Billaud D, Ghanbaja J, Lambert. Preparation of new antimony (0)/polyaniline nanocomposites by a one-pot solution phase method. J Synth Met. 2005;151:165–74.
7. Aleshin AN. Polymer nanofibers and nanotubes: charge transport and device applications. Adv Mater. 2006;18:17–27.
8. Wang SX, Sun LX, Tan ZC, Xu F, Li YS. Synthesis, characterization and thermal analysis of polyaniline (PANI)/Co_3O_4 composites. J Therm Anal Calorim. 2007;89:609–12.
9. Yoshimoto S, Ohashi F, Kameyama T. Characterization and thermal degradation studies on polyaniline-intercalated montmorillonite nanocomposites prepared by a solvent-free mechanochemical route. J Polym Sci B. 2005;43:2705–14.
10. Qi YN, Xu F, Ma HJ, Sun LX, Zhang J, Jiang T. Thermal stability and glass transition behavior of PANI/γ-Al_2O_3 composites. J Therm Anal Calorim. 2008;91:219–23.
11. Qi YN, Xu F, Sun LX, Zeng JL, Liu YY. Thermal stability and glass transition behavior of PANI/α-Al_2O_3 composites. J Therm Anal Calorim. 2008;94:553–7.
12. Song GP, Han J, Guo R. Synthesis of polyaniline/NiO nanobelts by a self-assembly process. Synth Met. 2007;157:170–5.
13. Tsocheva D, Zlatkov T, Terlemezyan L. Thermoanalytical studies of polyaniline 'Emeraldine base'. J Therm Anal Calorim. 1998;53:895–904.
14. Aracil I, Font R, Conesa JA, Fullana A. TG-MS analysis of the thermo-oxidative decomposition of polychloroprene. J Anal Appl Pyrolysis. 2007;79:327–36.
15. Onishi A, Thomas PS, Stuart BH, Guerbois JP, Forbes SL. TG-MS analysis of the thermal decomposition of pig bone for forensic applications. J Therm Anal Calorim. 2008;92:87–90.
16. Jakab E, Mészáros E, Omastová M. Thermal decomposition of polypyrroles. J Therm Anal Calorim. 2007;88:515–21.
17. Pielichowski K. Kinetic analysis of the thermal decomposition of polyaniline. Solid State Ionics. 1997;104:123–32.
18. Dash DK, Sahu SK, Nayak PL. Thermal degradation studies of substituted conducting polyanilines. J Therm Anal Calorim. 2006;86:517–9.